Journal of Electroanalytical Chemistry 938 (2023) 117444

Contents lists available at ScienceDirect

Journal of Electroanalytical Chemistry

journal homepage: www.elsevier.com/locate/jelechem

Electrochemistry and electrochemical assessment of host–guest complexation of substituted pillar[m]arene[n]quinones

R.V. Shamagsumova [a], T.N. Kulikova [a], A.V. Porfireva [a], D.N. Shurpik [b], I.I. Stoikov [b], A.M. Rogov [c], D.I. Stoikov [b], G.A. Evtugyn [a,d,*]

[a] Analytical Chemistry Department of Kazan Federal University, Kremlevskaya, 18, 420008 Kazan, Russian Federation
[b] Organic and Medicinal Chemistry Department of Kazan Federal University, Kremlevskaya, 18, 420008 Kazan, Russian Federation
[c] Interdisciplinary Center of Analytical Microscopy of Kazan Federal University, 18 Kremlevskaya Street, Kazan 420008, Russian Federation
[d] Analytical Chemistry Department, Chemical Technology Institute of Ural Federal University, 19 Mira Street, 620002 Ekaterinburg, Russian Federation

ARTICLE INFO

Keywords:
Pillarquinone
Pillar[5]arene
Host–guest complexation
Cyclic voltammetry
Carbon black
Tyrosine determination

ABSTRACT

Electrochemical behavior of pillar[n]arene[m]quinone (n + m = 5, n = 2–4) has been for the first time investigated in aqueous media on the glassy carbon electrode. All the compounds studied showed quasi-reversible redox conversion to hydroquinone derivatives. The reaction was not complicated with ionization of hydroxy groups or by the formation of intramolecular hydrogen bonds. In the whole pH region tested (2.0 – 9.0) the stoichiometry of electron and hydrogen ions transfer was found the same (1:1). The peak currents changed with no respect of the number of quinone units in the macrocycle molecule and were probably more affected by steric factors and self-aggregation confirmed by scanning electron microscopy. Adsorption of the macrocycles on the electrode covered with carbon black resulted in remarkable improvement of the conditions of electron exchange and of the peak currents on voltammograms. Screening of possible guest molecules showed that among amino acids, tyrosine formed complexes with pillarquinones both in solution and on the electrode interface. Complexation resulted in decrease of the peak currents on voltammograms due to steric hindrance of electric wiring. This made it possible to determine 5–100 μM tyrosine in the solution and 1–100 μM tyrosine with pillar[3]arene[2]quinone adsorbed in the carbon black layer. No interferences were established in normal human serum and Ringer-Locke's solution. The approach to supramolecular detection of small molecules by intrinsic redox activity of the macrocyclic hosts can be extended to other analytes by modification of the macrocyclic components of the reaction.

1. Introduction

Pillararenes first reported in 2008 by T. Ogoshi group [1] are new representatives of the macrocyclic compounds able to form host–guest complexes and hence affect the guest molecules properties assessed by various physical–chemical methods [2–5]. Pillararene molecules consist of 1,4-hydroquinone derivatives bridged with methylene groups in *para*-position and have a highly symmetrical pillar shaped architecture. Pillararenes capture neutral organic species in the cavity via multiple non-covalent C—H···π interactions [6,7]. Besides, they can form hydrogen bonds via unsubstituted hydroxyl groups or participate in electrostatic interactions involving charged substituents at the macrocyclic core [8,9]. The variety of specific interactions and the prospects of chemical modification of the macrocycles make pillar[n]arenes attractive for assembling chemical sensors [10–12]. In them, macrocycles play role of selective sorbents accumulating the analyte molecules in the proximity of the transducer interface. Impressive examples of such sensors have been published for sensitive detection of adrenaline [13], paraquat [14], trinitrotoluene [15], tryptophan [16], viologen derivative [17], caffeic acid [18], acetaminophen and dopamine [19], tryptophan [20,21], and methylamphetamine [22]. In some of them, self-assembling of the macrocycles into 3D organized structures has been employed to reach selectivity of recognition and sensitivity of an analyte detection. Besides, supramolecular composites based reduced graphene oxide modified with acetohydrazide derivatives of pillar[5]arene [24] and those assembled in polypyrrole film [25] have been successfully utilized in assembling supercapacitor electrodes. They exhibited high initial capacitance and excellent cycling stability. Deca-susbstituted pillar[5]arene with tertiary trimethylammonium groups was used as a nanocontainer for curcumin derivative

* Corresponding author at: Analytical Chemistry Department of Kazan Federal University, Kremlevskaya, 18, 420008 Kazan, Russian Federation.
E-mail address: Gennady.Evtugyn@kpfu.ru (G.A. Evtugyn).

https://doi.org/10.1016/j.jelechem.2023.117444
Received 5 February 2023; Received in revised form 7 April 2023; Accepted 8 April 2023
Available online 11 April 2023

and showed pH-dependent stability of the host–guest complex formed. This promises further application of such systems for targeted drug delivery systems [26]. In our previous research, we have demonstrated the prospects of pillararene based recognition systems in optic and electrochemical sensing of various guest molecules and broad possibilities offered by functionalization of the macrocyclic platform to reach selectivity and sensitivity of recognition event (see reviews [27–29]).

In most of the mentioned applications, target molecules involved in the interactions with the substituents and/or macrocyclic cavity generate the signal while pillararenes themselves remain unchanged. The use of the redox active guest signal can be utilized for electrochemical sensing of biologically active compounds even though they do not show their own active on the electrode [14]. To detect such species, pillararenes are first involved in the complexation with the redox probes, which are then released by substitution with the target species. As the reactivity of redox probes bonded and released from host-guest complex differs from each other, change observed can be used for quantification of the guest competing with the redox probe for the binding sites. This protocol is relative to the displacement technique described in immuno- and DNA-sensors [23,30–34]. Methylene blue, rhodamine and thionine have been employed to reach signals on antigen–antibody and DNA (aptamer) – analyte interactions.

Electrochemical sensors show undoubted advantages in the determination of small organic molecules in portable format, i.e., well developed theory, intuitively understandable interpretation of the measurement results, high sensitivity and acceptable selectivity of the response, inexpensive instrumentation, and moderate requirements to the stuff qualification. However, own redox activity of unsubstituted pillararenes in electrochemical sensing has found less attention than application of the redox active guests. This might be probably due to low stability of hydroxylated fragments of the macrocycles found in the investigation of perhydroxylated pillar[5]arene (P[5]A) [35] and pillar[6]arene [36]. They exist in aqueous solutions in semi-oxidized form even though special measures were taken to prevent their reaction with dissolved oxygen. Together with concerted formation/ distortion of the intramolecular hydrogen bonds system affecting the electron / hydrogen ion transfer, this complicates the involvement of the pillararenes in the electron exchange path on the electrode interface. It was also reported for P[5]A that its adsorption on glassy carbon electrode (GCE) resulted in the partial electrode passivation by intermediate oxidation products. For this reason, only few examples of the use of perhydroxylated pillararenes in the assembly of electrochemical sensors can be mentioned. Thus, they were utilized in mediated oxidation of thiocholine that is applied in acetylcholinesterase sensors for the detection of appropriate inhibitors [36]. Changes in the P[5]A redox properties were used for discrimination of native and damaged DNA adsorbed on GCE covered with carbon black [37].

Reversibility of the redox conversion of the hydroquinone and benzoquinone units in the pillar[n]arene molecules offers another way for assembling appropriate sensors and biosensors. The use of quinone derived macrocycles named pillar[n]arene[m]quinones makes it possible to start with reduction of quinone fragments to hydroquinone with significantly lower influence of hydrogen bonds and chemosorption of semiquinone units frequently observed in direct oxidation of relative pillar[n + m]arenes. Indeed, possibility of reversible P[5]A oxidation and similarity of appropriate voltammograms to those of hydroquinone were reported from very beginning of the pillararene chemistry [38]. Reversible conversion of quinone to hydroquinone and vice versa were reported for partially alkoxylated P[5]A [39] and pillar[6]arene [40]. Pillar[6]quinone was obtained by chemical and electrochemical oxidation of perhydroxylated pillar[6]arene [41]. Cathodic voltammetric studies showed stepwise transfer of electrons in reversed process. It should be noted that all of these examples describe electrochemical behavior of hydroxylated pillararenes in organic media. Due to low protogenic activity of the media, transfer of hydrogen ions becomes hindered, so that the products of one-electron transfer are visible on voltammograms, possible influence of hydrogen bonding is suppressed and that of supramolecular self-assembling increased against the conditions of aqueous or preferably aqueous solutions more convenient for electrochemical (bio)sensos operation. Nevertheless, partially oxidized pillararenes (pillarquinones) retain their ability to host–guest interactions [42]. It was shown on the example of potentiometric determination of some metal cations [43] and colorimetric detection of aliphatic aldehydes from their vapors [44]. However, to the best of our knowledge, there is no information on electrochemical behavior of pillarquinones in aqueous media, where hydrogen bonding of hydroquinone units can sufficiently affect both the redox activity of the macrocycle and its recognition capabilities toward potential guest molecules. For the first time, we have compared the electrochemical characteristics of the above macrocycles different in the number and location of quinone units in the macrocycle core. Besides, selective recognition of tyrosine was for the first time found and applied for its sensitive detection.

In this work, electrochemical properties of partially oxidized P[5]A with one, two, and three quinone units have been for the first time investigated in 50% acetone and on the surface of GCE covered with carbon black. Their abilities in recognition of amino acids have been compared and selective voltammetric detection of tyrosine demonstrated for pillar[3]arene[2]quinone demonstrated.

2. Materials and methods

2.1. Reagents

Chemical structures and notations of pillar[n]arene[m]quinone (n + m = 5, n = 2–4, m = 1–3) are presented in Fig. 1. They were synthesized at the Department of Organic and Medicinal Chemistry of Kazan Federal University in accordance with modified method [45].

First, P[5]A decasubstituted with 1,4-bis(2-bromoethoxy) groups **(1)** was synthesized in accordance with [46]. Cerium ammonium nitrate $(NH_4)_2[Ce(NO_3)_6]$ dissolved in minimal quantity of water was mixed with dichloromethane/tetrahydrofuran mixture 1:1 (v/v) to form homogeneous solution. The reaction was continued for 16 hr. The number of oxidized hydroquinone units depended on the molar ratio of the reactants. Thus, the addition of 2.2 mol of oxidant per one mol of 1,4-dibromoethoxy unit resulted in formation of P[4]Q[1], 4.4 mol of added oxidant preferably gave P[3]Q[2] and 6.6 mol allowed formation of P[2]Q[3] with the yields varied from 38 to 54% (Scheme 1).

The structure of all the obtained compounds including precursor was confirmed by ^{1}H, ^{13}C NMR spectroscopy IR spectroscopy, MALDI-TOF mass spectroscopy and elemental analysis (Electronic Supplementary Information, ESI, Figs. S1-S12). The number and position of quinone fragments in the macrocycles were established based on the ^{1}H and ^{13}C NMR spectra as described in ESI (Table S1).

Amino acids (L-asparagine, L-cysteine, L-glycine, L-histidine, DL-leucine, DL-methionine, L-phenylalanine, L-tryptophan, and DL-tyrosine) and choline were purchased from Sigma-Aldrich (Darmstadt, Germany). Normal human serum was purchased from ThermoFischer Scientific and rehydrated prior to use with phosphate buffer saline, pH 7.6. Ringer-Locke's solution contained 9 g/L NaCl, 0.42 g/L KCl, 0.5 g/L $NaH_2PO_4{\cdot}2H_2O$, 0.32 g/L $CaCl_2{\cdot}2H_2O$, 0.1 g/L $NaHCO_3$, 0.3 g/L $MgSO_4$, and 1.5 g/L D-glucose, pH 7.0.

Electrochemical measurements with dissolved macrocycles were performed in 0.04 M Britton-Robinson buffer mixed with acetone in 1:1 (v/v) ratio. Final solutions contained 0.1 M Na_2SO_4 as supporting electrolyte. All the solutions for electrochemical measurements were prepared using Millipore water (Simplicity® water purification system, Merck-Millipore, France).

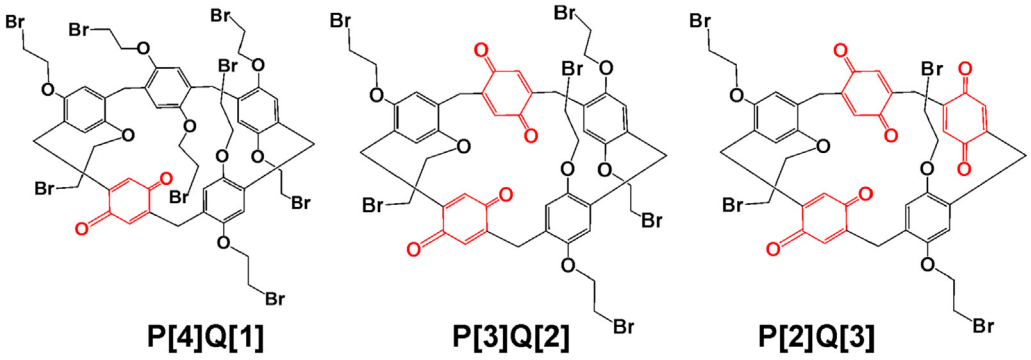

Fig. 1. Chemical structures of pillar[n]arene[m]quinones studied.

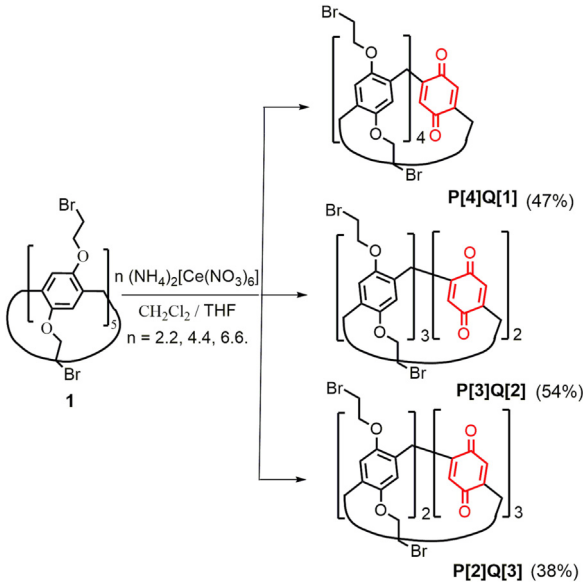

Scheme 1. Synthesis of pillarquinones.

2.2. GCE modification with pillar[5]arene quinones

GCE (2 mm in diameter) was mechanically polished, washed with acetone and deionized water and cleaned by repeated cycling of the potential in the range from −1.0 to 1.0 V until the voltammogram stabilization (approx. 10 min.). Carbon black (CB, N220, Imerys, Willebroek, Belgium) was suspended by sonication of 1 mg mL^{-1} dispersion in dimethylformamide. 4 μL of the suspension were drop casted on the GCE and dried at 60 °C for 30 min. Then, 2 μL of the macrocycles dissolved in acetone were casted on the surface and left drying at ambient temperature for 20 min.

2.3. Electrochemical measurements

Voltammetric measurements were performed with potentiostat/galvanostat AUTOLAB PGSTAT 302 N (Metrohm Autolab b.v., the Netherlands) at ambient temperature with three electrode working cell equipped with GCE as working electrode, double-junction Ag / AgCl / 3 M KCl reference electrode (Metrohm Autolab, the Netherlands) and Pt wire counter electrode.

The electrochemical impedance spectroscopy (EIS) measurements were performed using FRA2 module (Metrohm Autolab b.v., the Netherlands) in the presence of $[Fe(CN)_6]^{3-/4-}$ pair as the redox probe at the equilibrium potential calculated as a half-sum of the peak potentials of the redox probe. Frequency varied from 100 kHz to 0.04 Hz, amplitude of the applied sine potential was 5 mV. The EIS parameters (electron transfer resistance and constant phase element) were calculated from the Nyquist diagram with the R(RC)(RC) equivalent circuit using NOVA software (Metrohm Autolab b.v., Utrecht, The Netherlands).

2.4. Scanning electron microscopy measurements

Scanning electron microscopy (SEM) images were recorded on the field emission scanning electron microscope Merlin™ (Zeiss, Jena, Germany). The Au/Pd layer was deposited by T150ES sputter coater (Quorum Technologies Ltd, Laughton, UK).

3. Results and discussion

3.1. Electrochemical behavior of partially oxidized P[5]A

First, electrochemical properties of the oxidized partially substituted P[5]A were assessed in homogeneous conditions. Because of rather low solubility of the above compounds in water, all the working solutions contained 50 vol% acetone. Constant ionic strength was maintained by addition of Na_2SO_4 to its final concentration of 0.1 M. Previously it was found [37] that these conditions provide most reproducible peaks related to the perhydroxylated pillararene redox conversion. It should be mentioned that all the measurements were performed starting from maximal anodic potential corresponded to the stable quin one form and scanning the potential toward cathodic potentials corresponded to the fully reduced forms of the macrocycles. Full cyclic voltammograms recorded are shown in Figs. S13, S14. In the following text, the region of the peak pairs related to the reversible conversion of the quinone fragments has been selected for more clarity of the changes observed in variation of the measurement conditions.

Repeated cycling of the potential did not result in the pH changes of the solution and the peak potentials remained quite stable. All the measurements were performed in solutions containing dissolved oxygen. Its removal by argon did not alter main peak pair attributed to the benzoquinone/hydroquinone fragments conversion. Appropriate cyclic voltammograms of the P[3]Q[2] obtained for the macrocycle adsorbed on the electrode are presented in Fig. S13 as example.

All the macrocycles tested showed a pair of the peaks attributed to the reversible reduction of the quinone units of the macrocycle and reversed oxidation of hydroquinone fragments obtained (Fig. 2). Appropriate reaction is presented in the Scheme 2.

The parameters of the dependence of the peak currents (I_{pa} (I_{pc}), μA) on the macrocycle concentration (c, M) are presented in Table 1. The slope of the I_{pa} – c dependence was rather similar to each other within the confidence interval. The intercepts of all the regressions significantly differed from zero. This indicates contribution of surface accumulation of the molecules to the currents recorded.

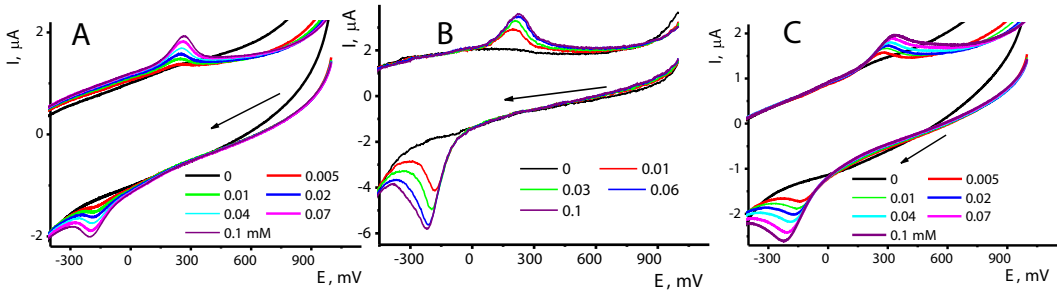

Fig. 2. Cyclic voltammograms recorded on the GCE in 0 – 0.1 mM P[4]Q[1] (A), P[3]Q[2] (B) and P[2]Q[3] (C), pH 5.0, scan rate 100 mV/s. Arrow indicate the direction of the potential scanning.

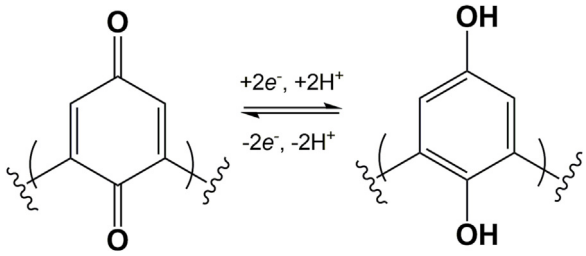

Scheme 2. General mechanism of reversible reduction–oxidation of quinone fragments in pillarquinone molecules.

One can see the peak currents did not directly depend on the number of quinone units per macrocycle molecule. Thus, maximal cathodic peak was observed for the P[3]Q[2] while other macrocycles showed comparable peaks. Anodic peaks on the reversed scan were much closer to each other than the cathodic peaks. This might result from combined influence of two factors, i.e., increasing number of the redox centers in a macrocycle and their accessibility to the electron transfer influenced by steric loading of the quinone units. In the case of P[2]Q[3] with three neighboring quinone units, the reduction reaction can be also complicated by stabilization of the formation of intramolecular hydrogen bonds in the intermediate products of reduction. However, this hypothesis contradicts with similarity of the peak potentials and a single step electron transfer, i.e., formation of the only peak pair for all the compounds studied. The highest cathodic peaks of the P[3]Q[2] demonstrated the deepest diffusion decay among all the compounds studied. It should be also noted that only P[4]Q[1] gave about similar oxidation and reduction peak currents ($I_{pc}/I_{pa} \approx 1$) whereas other macrocycles showed much higher cathodic peak over anodic one. This indirectly confirms a significant contribution of the surface confined steps to the oxidation of hydroquinone units formed at the direct scan of the potential.

The dependence of the peak currents (I_p) on the scan rate (ν) corresponded to the mixed regime of adsorption/diffusion control (Table S2). For all the compounds studied the slopes in bi-logarithmic plots, dlog(I_p, μA)/dlog(ν, mV/s) approached to 1 (surface confined reaction) for anodic peaks and were much lower for cathodic peaks (near 0.75 for P[4]Q[1], 0.67–0.75 for P[3]Q[2] and 0.60–0.84 for P[2]Q[3]). The deviation of appropriate values was higher for P[2]Q[3] among the macrocycles and that measured at pH 7.0 among other buffers. At higher pH values, the appropriate dependences become non-linear by downward against linear dependency at high scan rates.

The pH dependence of the cyclic voltammograms of the macrocycles is presented in Fig. 3 for P[3]Q[2] as an example and in Figs. S14 and S15 for P[4]Q[1] and P[2]Q[3], respectively. Equilibrium potential E_{eq} was calculated as a half-sum of the peak potentials (1). In accordance with its value, equal number of hydrogen ions and electrons is transferred for all the compounds studied ((2)–(4)).

$$E_{eq} = \left(E_{pa} - -E_{pc}\right)/2 \quad (1)$$

$$P[4]Q[1] : E_{eq}320 = (.1 \pm 7.5) - -(52.3 \pm 1.3)pH, n = 8, R^2 = 0.9959 \quad (2)$$

$$P[3]Q[2] : E_{eq} = (324.9 \pm 8.9) - -(53.8 \pm 1.5)pH, n = 8, R^2 = 0.9945 \quad (3)$$

$$P[2]Q[3] : E_{eq} = (322.7 \pm 6.9) - -(52.7 \pm 1.3)pH, n = 8, R^2 = 0.9965 \quad (4)$$

The peak currents weakly depended on the pH. For P[4]Q[1], reduction peak current remained about constant in the range of pH from 2.0 to 7.0 and slightly increased with pH 8.0–9.0. The increase of the currents can be attributed to the alternative oxidation of quinone units by dissolved oxygen, which reactivity is higher in basic media. Anodic peak current regularly decreased in the range from

Table 1
The dependency of the peak currents (I_p, μA) on the concentration of pillar[n]arene[m]quinones (c, μM) I_p = (a ± Δa) + (b ± Δb)·c, n is the number of experimental points within the linear range.

Pillar[n]arene[m]quinone	a ± Δa	b ± Δb	n	R^2	Conc. range, μM
P[4]Q[1]	Oxidation peak current				
	0.078 ± 0.004	2.90 ± 0.05	5	0.9981	20–100
	Reduction peak current				
	0.021 ± 0.007	3.74 ± 0.09	7	0.9991	0.1–100
P[3]Q[2]	Oxidation peak current				
	0.62 ± 0.10	5.26 ± 1.71	7	0.9022	0.01 – 0.10
	Reduction peak current				
	1.89 ± 0.15	26.1 ± 4.1	5	0.9529	0.01 – 0.06
P[2]Q[3]	Oxidation peak current				
	0.53 ± 0.04	7.55 ± 0.71	5	0.9732	0.02 – 0.10
	Reduction peak current				
	0.31 ± 0.02	0.86 ± 0.12	5	0.9253	0.02 – 0.10

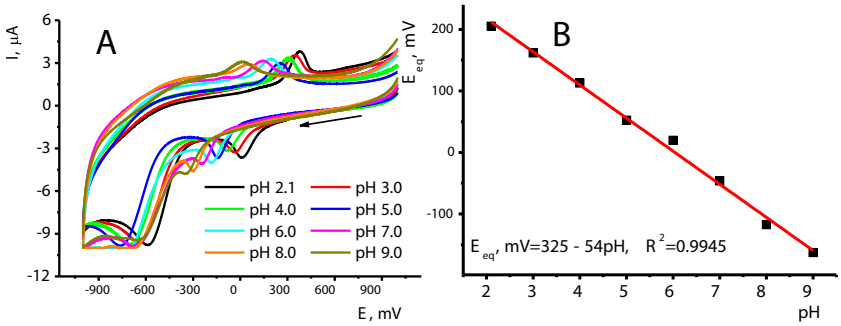

Fig. 3. Cyclic voltammograms of 0.1 mM P[3]Q[2] (A) and pH dependence of the equilibrium potential E_{eq} calculated from the peak potentials (B). Average from six measurements with individual electrodes.

pH 2.0 to 9.0 by about 25% of its maximal value. Similar trends were observed for other macrocycles. Thus, P[3]Q[2] showed linear dependencies of the anodic peak current within the whole range of the potentials mentioned with the slope $dI_{pa}/dpH = -0.19 \pm 0.02$ Cathodic peaks showed a local increase in the neutral media and the same values in acidic and basic solutions. Here, two neighboring quinone units stabilize semi-oxidized form by internal hydrogen bonding so that the currents were less sensitive to the oxygen presence. For P[2]Q[3], oxidation peak current was much less sensitive to the pH ($dI_{pa}/dpH = -0.079 \pm 0.002$) whereas cathodic peak current increased twofold in the pH range from 2.0 to 6.0 and stabilized in more basic conditions. Probably, deprotonation increased the number of quinone units involved in electrode reaction against those active in acidic media stimulating hydrogen bonding of benzoquinone-hydroquinone units. Appropriate dependencies are presented in Fig. S14.

The transfer coefficients (α) and heterogeneous reaction rates (k) of the electron transfer were calculated from the slopes of the dependencies of the peak current on the scan rate (5) [47].

$$E_{pa} = E^{0'} + \frac{2.303RT}{(1-\alpha)nF}\log\frac{(1-\alpha)nF}{RTk_s} + \frac{2.303RT}{(1-\alpha)nF}\log\nu$$
$$E_{pc} = E^{0'} + \frac{2.303RT}{\alpha nF}\log\frac{RTk_s}{\alpha nF} - \frac{2.303RT}{\alpha nF}\log\nu \quad (5)$$

$E^{0'}$ is the formal redox potential, R universal gas constant, T absolute temperature, n the number of electrons transferred, F the Faraday constant, and k_s the heterogeneous constant rate of the electron transfer. Appropriate curves in the plots E_p – logν are presented in Fig. S16 and kinetic parameters of the electron transfer in Table 2. All the compounds showed the transmission coefficient increased with pH from about 0.5 to 0.7 indicating higher contribution of chemical steps with intermediate products of electron transfer. Contrary to that, oxidation showed much lower pH influence. P[2]Q[3] showed non-linear dependence of the E_{pc} on logν with two linear pieces at lower and higher scan rates. As could be seen, transmission coefficient did not depend on pH at lower scan rates (5 – 200 mV/s) and significantly decreased at faster runs (150 – 500 mV/s). Thus, the α_c value shifted in opposite direction with pH against other macrocycles indicating higher contribution of intermolecular processes probably involving hydrogen bonding of hydroquinone and quinone units of the macrocycle.

The performance of partially oxidized P[5]A molecules coincides with the redox behavior of substituted quinones but differs from that of sterically hindered anthracyclines and anthraquinones that show separate steps of electron/H^+ ions transfer on voltammograms (see review [48]). Increased pH did not result in splitting the peaks on voltammograms due to ionization of hydroxy groups of the reduction products as was shown for substituted quinones in non-buffered media [49]. It seems from the experiments, that steric factors affecting the access of the pillarquinone molecules to the electrode mostly determine the behavior of the compounds studied and similarity of the anodic peaks on reversed runs on voltammograms with no respect of the number of quinone units in the initial compounds. Only P[2]Q[3] with three neighboring quinone groups offers possibility of intermolecular hydrogen bonding on semi-oxidized intermediates similarly to quinhydrone complex on hydroquinone and benzoquinone molecules [50].

3.2. Electrochemical behavior of pillarquinones on the CB modified GCE

GCE was covered with the CB layer, and inert and inexpensive carbon nanomaterial with high adsorption capacity and good mechanical and electrical properties. CB is frequently applied for enhancement of the working area of electrodes and electric wiring of biomolecules in electrochemical sensors and biosensors [51]. The concentration of the CB dispersion and protocol of its deposition were specified elsewhere [35] and corresponded to the full coverage of the GCE surface. Fig. 4 shows surface morphology of the CB covered GCE prior to and after the deposition of the P[3]Q[2] to the GCE modified with CB.

The aliquot was chosen to be 4 μL per electrode while the concentration of the macrocycle varied from 0.1 mM to 10 mM. At lowest concentration, the macrocycle forms a thin dense film that fully covers the CB particles remained visible on the image. With increased P[4]Q[2] concentration, regularly shaped round plaques appeared onto the film. The following increase of the macrocycle concentration resulted in increase of both the number and diameter of the plaques till their domination at 10 mM P[4]Q[2]. EDX elemental analysis confirmed presence of P[4]Q[2] indicated by bromine content both in the film and plaques (Figs. S17, Table S3).

Effective surface area of the modified electrode was estimated by the Randles-Ševcik equation (6) using 1.0 mM $K_3[Fe(CN)_6]$ with its diffusion coefficient of 7.6×10^{-6} cm^2 s^{-1} [52].

$$I_p = 2[\text{unknown template}] \quad (6)$$

Roughness coefficient as a ratio of real and geometric electrode areas was equal to 1.7. This coincides well with previously reported data [30].

Introduction of pillarquinones in the CB layer was confirmed by EIS. Fig. 5 represents the Nyquist diagrams obtained in the presence of 10 mM $[Fe(CN)_6]^{3-/4-}$ as redox probe on the electrodes consecutively loaded with CB and pillarquinones studied.

Appropriate parameters are summarized in Table S4. Semicircles on the Nyquist diagram corresponded to the limiting step of the electron transfer on the inner (electrode – modifier) and upper (modifier – solution) interfaces (see equivalent circuit in (7). Here, R_s is the solvent resistance, R_{et} the electron transfer resistance and C is the constant phase element. Indices '1′ and '2′ correspond to inner (electrode – modifier) and outer (modifier – solution) interfaces of the electron exchange.

Table 2
Transfer coefficient (α) and heterogeneous rate constant of the electron transfer (k_c, k_a). Average ± S.D, three repetitions.

pH	α	k_c	1-α	k_a
P[4]Q[1]				
3.0	0.56	0.016 ± 0.002	0.67	0.0073 ± 0.0013
5.0	0.61	0.008 ± 0.0006	0.62	0.0081 ± 0.0006
7.0	0.75	0.003 ± 0.001	0.52	0.0164 ± 0.0034
P[3]Q[2]				
3.0	0.53	0.0333 ± 0.0019	0.57	0.026 ± 0.0019
5.0	0.59	0.0230 ± 0.0013	0.65	0.014 ± 0.0023
7.0	0.67	0.0132 ± 0.0014	0.57	0.025 ± 0.006
P[2]Q[3]				
3.0	0.66 (5 – 200 mV/s)	0.0025 ± 0.0001	0.64	0.0026 ± 0.0005
	0.40 (150 – 500 mV/s)	0.029 ± 0.002		
5.0	0.60 (5 – 200 mV/s)	0.0020 ± 0.0002	0.52	0.0036 ± 0.0007
	0.30 (150 – 500 mV/s)	0.049 ± 0.004		
7.0	0.60 (5 – 200 mV/s)	0.0019 ± 0.0002	0.52	0.0035 ± 0.0005
	0.29 (150 – 500 mV/s)	0.052 ± 0.005		

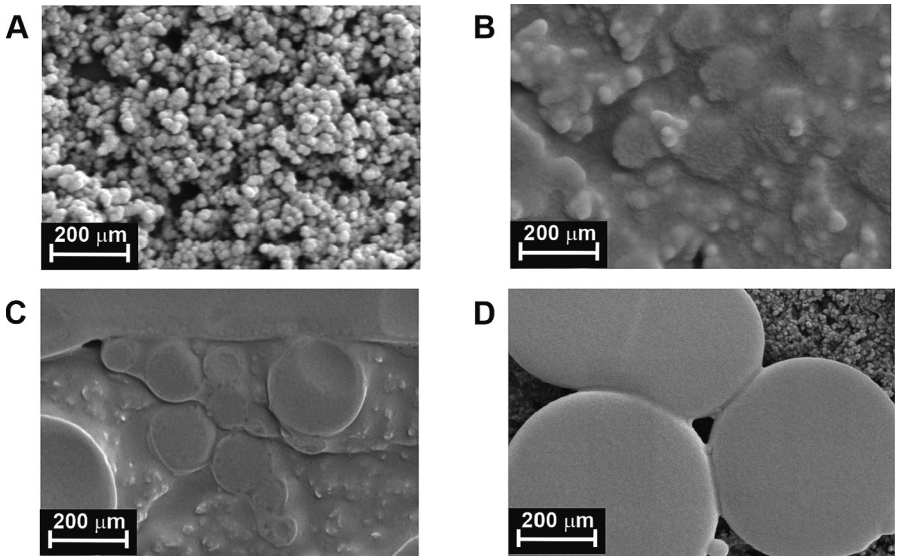

Fig. 4. SEM images of the GCE covered with CB (A) and that after deposition of 0.1 mM (B), 1.0 mM (C) and 10 mM P[3]Q[2] (D).

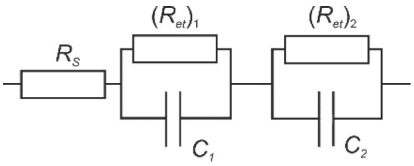

The exponential factor N (Eq. (8), Z is an impedance, ω angular frequency of a sinusoidal signal, and $j^2 = -1$) was higher than 0.98 in all the measurements indicating the behavior of constant phase elements as an ideal capacitance.

$$Z = \frac{1}{(j\omega)^N C} \tag{8}$$

Deposition of all the macrocycles did not alter the electron transfer resistance of the electrode - modifier interface but increased two-threefold its capacitance. Regarding outer interface, deposition of P[4]Q[1] did not affect the EIS parameters while the addition of P[3]Q[2] decreased and P[2]Q[3] increased the R_{et} value by about 10–12%. The capacitance changed in the opposite direction against R_{et} trend indicating higher charge separation in case of P[3]Q[2] and lower one for P[2]Q[3].

On cyclic voltammograms, all the GCEs modified with the macrocycles adsorbed in the CB layer showed one pair of quasi-reversible redox peaks, which morphology was similar to that obtained on bare GCE with dissolved macrocycles. Meanwhile, the shape of the peaks differed, especially for P[4]Q[1] and P[2]Q[3]: all the peaks obtained on the modified electrodes have a remarkable diffusional decay and looked like classical diffusion controlled peaks though the redox active species were in the surface layer but not in the solution. The signals

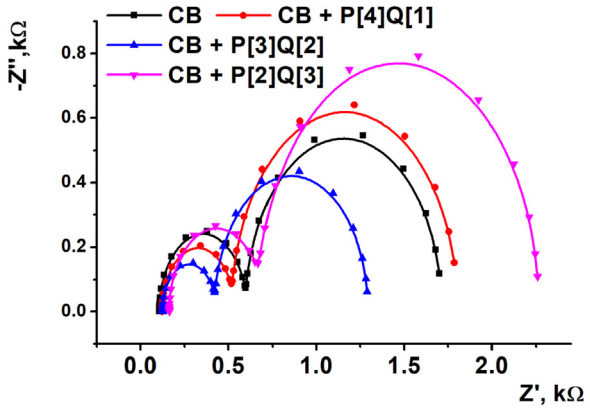

Fig. 5. The Nyquist diagrams obtained on GCE covered with CB and pillarquinones studied. Measurements in the presence of 10 mM $[Fe(CN)_6]^{3-/4-}$.

attributed to the redox reactions of the macrocycles reached stable currents to third-fourth cycle of the potential with intermediate stirring of the solution. The appropriate cyclic voltammograms were quite stable in the following measurements within at least one day. It should be noted that contrary to the same macrocycles dissolved in aqueous acetone, the same compounds adsorbed on the CB particles were also stable in basic media, so that the voltammograms recorded at pH 8.0 were well reproducible. This can result from stabilization of the macrocycles and their reduction products in the matrix of nanomaterials and less accessibility of the adsorbed molecules of pillarquinones for oxygen molecules on the electrode interface.

The height of both cathodic and anodic peaks was much higher than that reached in homogeneous conditions (see Section 3.1). The ratio of cathodic and anodic peak currents was closer to one at all of the pH of the media (Fig. 6). The peak potentials depended on the pH of the solution in accordance with Eqs. ((9)–(11)).

$$P[4]Q[1]/CB: E_{eq} = (267.4 \pm 13.2) - -(48.0 \pm 2.2)pH, n = 8, R^2 = 0.9852 \quad (9)$$

$$P[3]Q[2]/CB: E_{eq} = (347.3 \pm 4.5) - -(52.6 \pm 1.2)pH, n = 8, R^2 = 0.9986 \quad (10)$$

$$P[2]Q[3]/CB: E_{eq} = (499.9 \pm 20.5) - -(86.4 \pm 3.5)pH, n = 8, R^2 = 0.9915 \quad (11)$$

Super-Nernstian response of the dependency observed for P[2]Q[3] can be explained by the pH influence on the disaggregation processes and increased number of proton accepting groups o the electrode interface. It should be noted that the P[2]Q[3] macrocycle is the only one able to form hydrogen bonds in semi-oxidized state among the compounds tested. This suggestion coincides with a sharp increase of the reduction peak current observed for this compound in the pH range from 6.0 to 9.0. (Fig. 7) Other compounds showed rather smoothen plots which did not significantly differ from those obtained with dissolved macrocycles.

Increasing quantities of the macrocycles loaded onto the CB layer resulted in remarkable increase of the peak currents of pillarquinones till deposition of 100–200 nmol per electrode. Fig. 8 shows the appropriate cyclic voltammograms for P[3]Q[2] as example.

The loading of other macrocycles was characterized in a similar manner in Fig. S18. As could be seen, at pH 8.0 the assessment is complicated by amalgamation of the peaks related to the oxygen and quinone units' reduction. This resulted in apparent increase of the cathodic peak currents which become much less sensitive to the macrocycle loading than at pH 5.0. The effect is most obvious for P[2]Q[3] but also affects the cyclic voltammograms of P[2]Q[3]. In case of P[3]Q[2], joint cathodic process is observed only at highest quantities of the macrocycle loaded on the GCE/CB surface. The difference in the behavior of various pillarquinones can be related to their self-assembling on the electrode as previously was confirmed by SEM for the P[3]Q[2] and indirectly by EIS data. The formation of aggregates not only alters the surface concentration of redox sites but also influences the hydrophobicity of the electrode interface and hence the rate of hydrogen ion transfer in the surface layer. These phenomena can explain the decrease of the currents observed in some measurement conditions at high quantities of the macrocycles loaded.

Electrode kinetics of redox reactions on the GCE/CB electrode was assessed for adsorbed pillarquinones as described above for their solutions. The transfer coefficients and heterogeneous rate constants are presented in Table 3. In comparison with homogeneous conditions (Table 2), the transfer coefficients of the direct reaction (cathodic reduction of quinone units) are closer to 0.5 indicting higher reversibility of the electron exchange. Appropriate rate constants also increased eight- tenfold against those obtained with the macrocycle solutions. This might result from better electric wiring of the macrocycle molecules adsorbed on the CB particles in comparison with their transfer to bare GCE. As in the case of solution testing, P[2]Q[3] exerted lower changes of the peak potentials with the scan rate, which are approximated with two linear pieces corresponded to different ranges of the variable. At higher scan rates, the transfer coefficient shifted to appr. 0.5 value and the constant rate increased ninefold indicating less influence of intermediate chemical streps of the reaction involving semi-oxidation products of the macrocycle conversion.

Thus, the results obtained show remarkable improvement of the voltammetric signals of pillarquinones after their deposition on the CB layer. Higher peak currents, comparable height of the cathodic and anodic peaks, their stabilization especially in basic media and lower contribution of oxygen reduction offer good opportunities for the use of pillarquinones as mediators in the assembly of electrochemical sensors. The above-mentioned improvements confirmed by changes in the kinetics of electron transfer can be attributed to the partial elimination of steric factors suppressing direct electron transfer to the pillarquinone molecule in the solution and a denser contact between the CB particles and redox sites of the molecules. Contrary to these positive factors.

3.3. Electrochemical detection of host–guest interactions with pillarquinones

3.3.1. Screening interactions of the amino acids with pillarquinones

As was mentioned in Introduction, the formation of host–guest complexes with derived pillararenes is mostly based on weak multiple interactions either with the aromatic rings of the macrocycle cavity or with functional groups of the substituents. Nitrogen containing derivatives can interact with oxygen atoms of both hydroquinone and benzoquinone units by donation of a lone electron pair or electrostatic interactions after protonation. We have performed screening of such interactions with primary amino acids and monitored changes in the redox behavior of the pillarquinones studied in the presence of amino acids. It is important that all the amino acids tested were electrochemically inactive and the voltammetric response could be attributed only

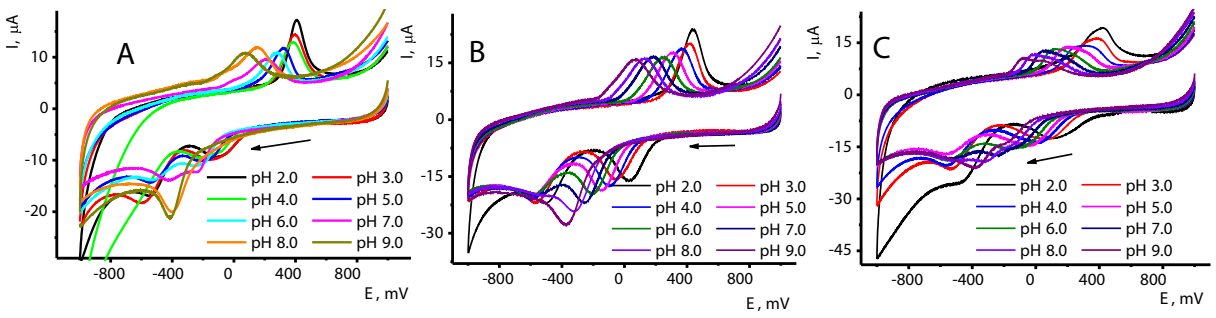

Fig. 6. Cyclic voltammograms recorded on GCE covered with CB and adsorbed macrocycles P[4]Q[1] (A), P[3]Q[2] (B) and P[2]Q[3] (C). Arrow indicates the direction of the potential scanning.

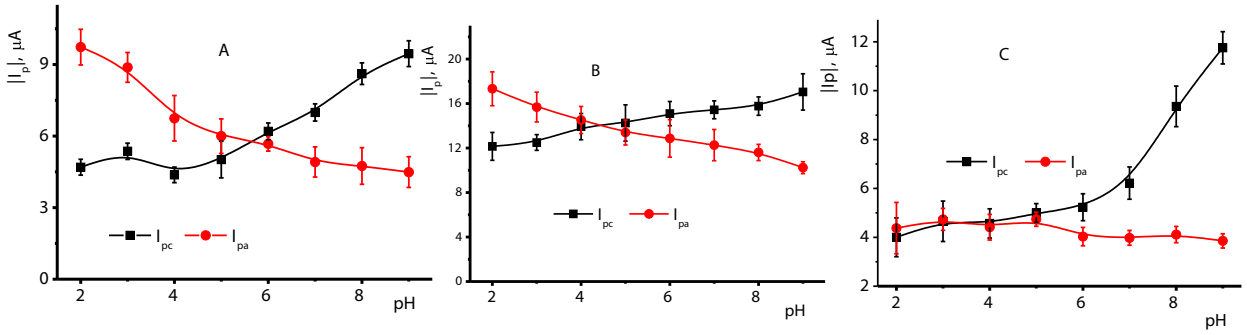

Fig. 7. The pH dependence of the cathodic (I_{pc}) and anodic (I_{pa}) peak currents of the GCE modified with CB and macrocycles, scan rate 100 mV/s.

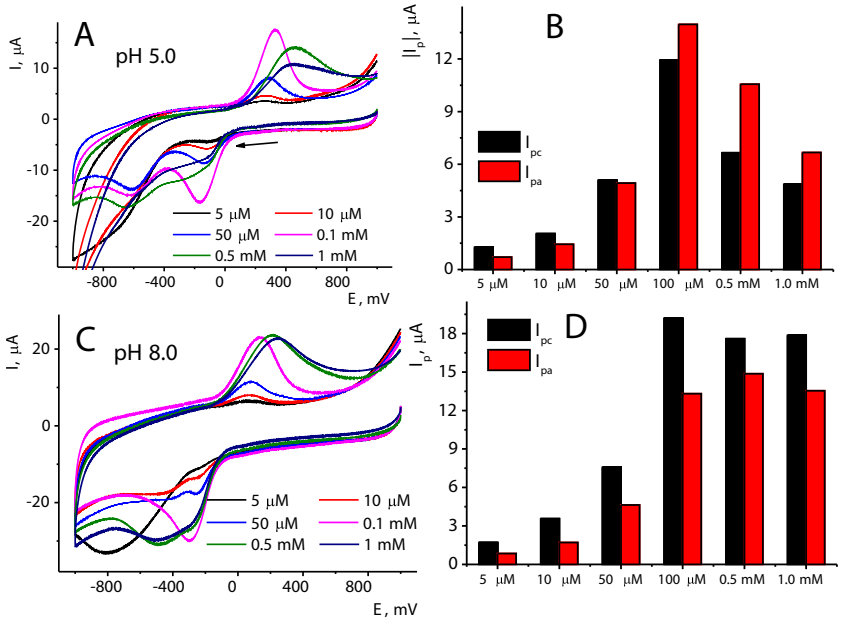

Fig. 8. Cyclic voltammograms (A, C) and peak currents (B, D) of 5 μM – 1 mM P[3]Q[2] at pH 5.0 (A, B) and 8.0 (B, D) recorded on the GCE covered with CB.

Table 3
Transfer coefficients (α) and heterogeneous rate constant of electron transfer (k_a, k_b). GCE modified with CB and adsorbed macrocycles. Average ± S.D, three repetitions.

pH	α	k_c	1-α	k_a
P[4]Q[1]				
3.0	0.62	0.016 ± 0.002	0.40	0.036 ± 0.001
5.0	0.59	0.0083 ± 0.0006	0.52	0.052 ± 0.001
7.0	0.43	0.0034 ± 0.0011	0.90	0.114 ± 0.004
P[3]Q[2]				
3.0	0.45	0.044 ± 0.004	0.50	0.033 ± 0.003
5.0	0.45	0.038 ± 0.003	0.42	0.042 ± 0.006
7.0	0.46	0.057 ± 0.006	0.39	0.085 ± 0.010
8.0	0.46	0.041 ± 0.006	0.37	0.075 ± 0.010
P[2]Q[3]				
3.0	0.71	0.027 ± 0.003	0.57	0.049 ± 0.005
	0.45	0.107 ± 0.004		
5.0	0.68	0.035 ± 0.011	0.34	0.186 ± 0.039
7.0	0.71	0.0544 ± 0.013	0.33	0.337 ± 0.063
8.0	0.64	0.0409 ± 0.009	0.31	0.252 ± 0.029

to the pillarquinones as host molecules exerting redox activity. Previously, substituted pillararenes have been described for amino acids recognition with electrochemical detection. In them, supramolecular complexes were applied for selective accumulation of the analytes followed by their oxidation on the electrode (tryptophan determination [16]). Fluorescent detection of amino acids binding is mostly based on displacement protocol with fluorescent dye as a guest substituted with amino acids. We have monitored the interaction of the pillarquinones studied with amino acids in solution. The concentrations of reactants were 0.1 mM for pillarquinones and 0.5 mM for potential

guests. Tryptophan was taken in 0.1 mM concentration due to lower solubility in the aqueous media. In most cases, the presence of amino acids did not alter the peaks on pillarquinone voltammograms. Some examples are given in Fig. S20. Among all the amino acids studied and pillarquinones, only tyrosine significantly affected the peak currents of P[3]Q[2] (Fig. 9).

In acidic media, the effect is much more pronounced for cathodic peak current that for anodic peak current. This coincides well with the positive charge of the guest molecule and predominant influence of the complexation on the protonation step within the reduction of the quinone units of the macrocycle. In neutral and basic media, changes of cathodic and anodic peak currents became comparable and the changes in the anodic peak were mostly related to the background currents indicating a higher resistance of the macrocycle complex on the electrode interface. The tyrosine presence did not affect the peak potentials in the whole range of the guest concentrations and pH varied. Probably, hydrophobic interactions with π-aromatic system of the amino acid molecule also plays role in binding to pillarquinone moiety. Introduction of guest molecule resulted in increased steric hindrance of the transfer of the host–guest complexes to the electrode surface and lower surface concentration of the same redox sites against blank experiments with no amino acids in the solution.

All the pillarquinones studied showed similar trends in the peak current alterations but the highest response was obtained for P[3]Q[2] (Fig. 10). In optimal conditions, the following calibration equations were obtained (Eqs. (12)–(15)). Th whole calibration curves were non-linear but can be approximated by two linear pieces at lower and higher tyrosine concentration range.

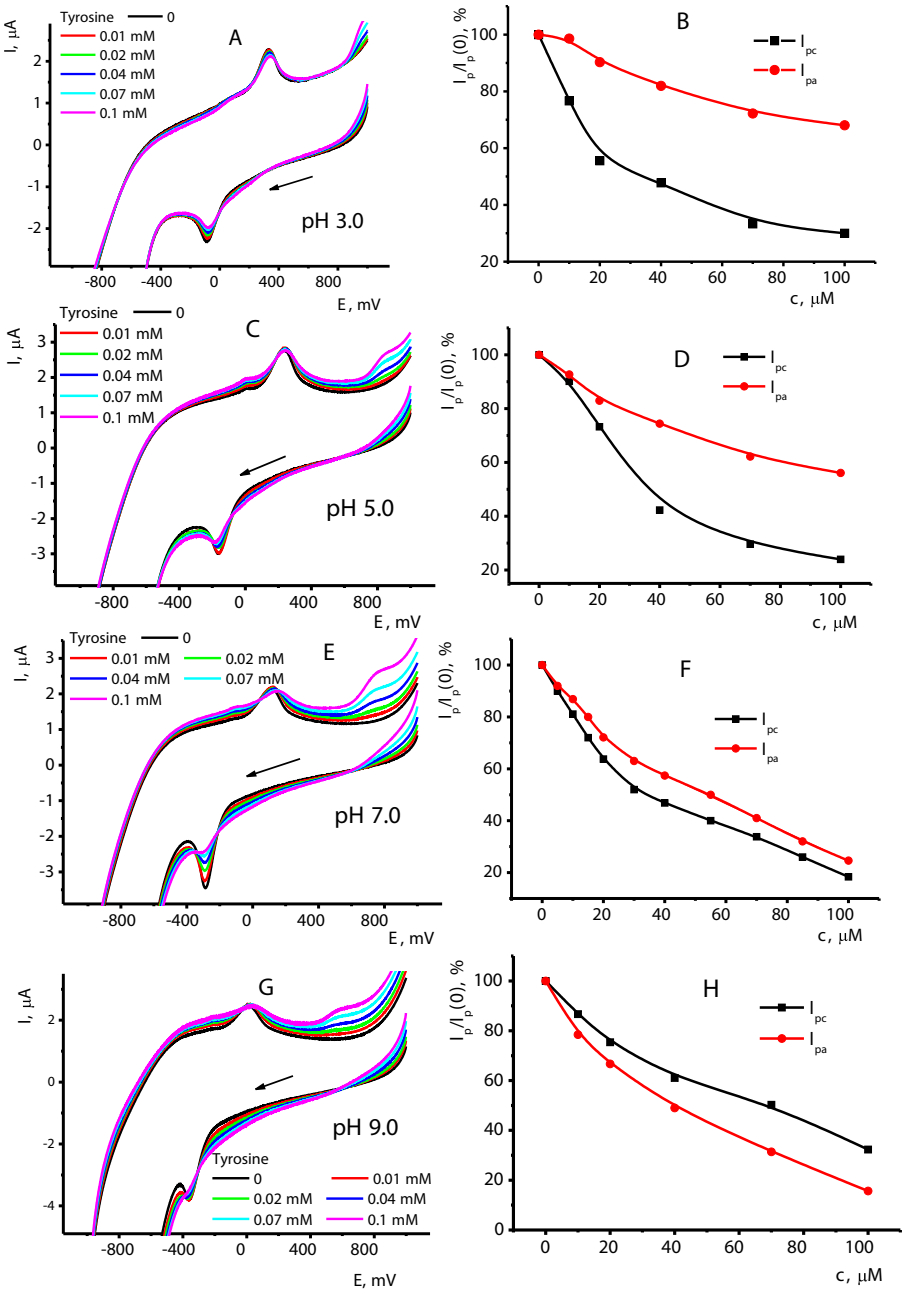

Fig. 9. Cyclic voltammograms (A, C, E, G) and peak currents (B, D, F, H) of the macrocycles adsorbed on the CB layer on GCE at various pH and tyrosine concentrations.

Cathodic peak currents:

$$5 - -30\mu M : I_{pc}/I_{pc}(0), \mu A = (98.0 \pm 1.4) - -(1.6 \pm 0.08)(c, \mu M), n = 5, R^2 = 0.9858 \quad (12)$$

$$30 - -100\mu M : I_{pc}/I_{pc}(0), \mu A = (66.2 \pm 0.4) - -(0.47 \pm 0.01)(c, \mu M), n = 6, R^2 = 0.9985 \quad (13)$$

Anodic peak currents:

$$5 - -30\mu M : I_{pa}/I_{pa}(0), \mu A = (98.9 \pm 0.9) - -(1.2 \pm 0.06)(c, \mu M), n = 5, R^2 = 0.9897 \quad (14)$$

$$30 - -100\mu M : I_{pa}/I_{pa}(0), \mu A = (79.8 \pm 0.6) - -(0.55 \pm 0.01)(c, \mu M), n = 6, R^2 = 0.9988 \quad (15)$$

The above changes were quite reproducible (R.S.D. of 4.5% for cathodic peaks and 5.5% for anodic peaks, six individual sensors) and did not depend on the period of incubation of the electrode mixture of the macrocycles and tyrosine. The sequence of reactant addition did not alter the resulting shift of the peak currents though the repeatability of the relative shift of the currents was higher in case of one-step addition of the mixture over to consecutive addition of the macrocycles and then tyrosine. The limit of detection (LOD) determined from S/N = 3 ratio was found to be 2 μM.

3.3.2. Determination of tyrosine with GCE modified with CB and P[3]Q[2]

After screening the conditions of host–guest complexation, the experiments were performed with the P[3]Q[2] implemented in the CB layer on the GCE surface. In the presence of tyrosine, the peak currents decreased as was previously described for homogeneous solutions. The concentrations detected were lower than those established with dissolved macrocycle though maximal relative decrease of the peak current was significantly lower (up to 40%) (Fig. 10).

Changes of anodic peak currents on reversed run on voltammogram were significantly lower than those of cathodic peak and rather irregular. Washing of the electrode after the contact with tyrosine resulted in changing the voltammograms to those obtained in blank measurement. However, the recovery of the sensor was not full and recorded peak currents diminished by 10–12% of initial value after each measurement. To avoid this memory effect, it was proposed to load the mixture of P[3]Q[2] and tyrosine on the GCE/CB surface. After preliminary washing of the electrode, such a protocol improved the reversibility of the peak changes and allowed performing tyrosine measurements for at least four days without renewing of the surface layer (up to ten measurements per day). Calibration curve was obtained for the shift of the cathodic peak current against blank experiment ΔI_{pc} against tyrosine concentration and was approximated with two linear pieces corresponded to low (1 – 10 μM) and high (10 – 100 μM) concentrations of tyrosine ((16), (17)).

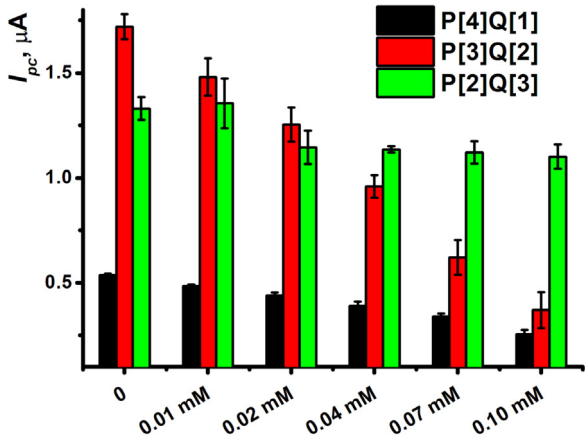

Fig. 10. Comparison of the cathodic peak current measured in the mixture of 0.1 mM pillarquinones and various concentrations of tyrosine a pH 7.0.

$$1 - -10\mu M : \Delta I_{pc}, \mu A = (4.12 \pm 0.6) - -(0.52 \pm 0.08)(c, \mu M), n = 5, R^2 = 0.9611 \quad (16)$$

$$30 - -100\mu M : \Delta I_{pc}, \mu A = (8.1 \pm 0.2) - -(0.08 \pm 0.003)(c, \mu M), n = 6, R^2 = 0.9923 \quad (17)$$

The LOD was equal to 0.4 μM. Tyrosine is an amino acid necessary for maintaining nutritional balance. It is involved in the synthesis of neurotransmitters, e.g., dopamine, norepinephrine, epinephrine, and L-dopa through a series of biochemical reactions. Tyrosine concentration is required in diagnostics of Parkinson's disease, depression and emotional disorders or dysfunction [53]. Tyrosine is mainly determined in body fluids using HPLC – MS [54], HPLC with fluorescence detection [55], capillary zone electrophoresis [56] and spectrometry [57]. Electrochemical methods offer an attractive alternative to conventional instrumentation due to low cost of equipment, simple operation, high sensitivity and user-friendly design. Characteristics of electrochemical determination of tyrosine with electrochemical sensors are compared in Table S5. Besides, some comprehensive reviews devoted to electrochemical detection of amino acids can be recommended [58,59]. As could be seen, the LOD obtained with the sensor developed is comparable with that achieved with other electrochemical sensors. Certainly, application of some nanomaterials and especially of graphene derivatives and nanocomposites offers higher sensitivity of the signal toward tyrosine. Meanwhile it should be mentioned that all the sensors described in the literature utilize direct or mediated oxidation of tyrosine accumulated on the modifier and hence are operated at rather high potential. This limits application of the sensors with rather simple samples which do not contain considerable amounts of oxidizable auxiliary agents or sample components or assumes complicated sample treatment. Application of pillarquinones made it possible to measure the signal in cathodic area, where no common interferences complicate the response.

3.3.3. Measurement precision, selectivity and real sample analysis

The electrochemical sensor based on GCE covered with CB/P[3]Q[2] showed high stability of the signal toward tyrosine. Thus, relative standard deviation determined for six consecutive measurements was equal to 4.5% (10 μM tyrosine, sensor-to-sensor repeatability). When stored at ambient temperature in working buffer, the sensor retains its characteristics within four days. Operation period can be extended by using relative changes of the cathodic peak current instead of absolute shift. The selectivity of tyrosine recognition was assessed for other amino acids (L-asparagine, L-cysteine, L-glycine, L-histidine, DL-leucine, DL-methionine, L-phenylalanine, L-tryptophan) and choline. It was found that in all the cases the shift of the P[3]A[2] peak currents in the presence of equal concentration of interferences did not exceed 2%. Besides, the same species were added to the 0.1 mM tyrosine and no alteration of the peak currents was observed, either.

Applicability of the sensor for real sample analysis was proved by using normal human serum rehydrated with phosphate buffer and spiked with 2.5 and 5 μM tyrosine. The recovery assessed by calibration curve for cathodic peak current shift was found to be 92 ± 5% and 110 ± 5, respectively (six sensors). No influence of Ringer-Locke's solution mimicking electrolyte content of the serum [60] on the response was also mentioned (recovery 99 ± 3% for three sensors).

4. Conclusion

The redox conversion of partially oxidized pillar[5]arenes containing from one to three quinone units is sterically hindered. The pH dependence of the equilibrium potential was linear in the pH range from 2.0 to 9.0 indicating no significant influence of the protonation-deprotonation on the electron transfer. Being transferred to the electrode interface by adsorption in the CB layer, piullarquinones retained reversibility of the electrode reaction. EIS and SEM indicated the formation of aggregates, which reactivity in the electrode reaction differed from that of individual molecules. In case of the P[2]Q[3], the whole redox reaction was additionally influenced by the hydrogen bonding. Searching guest molecules able to alter the redox behavior of the pillarquinones showed specific binding of tyrosine that partially suppressed the peak current on the voltammograms. No other amino acids tested exerted such an effect. Thus the signal toward tyrosine was achieved by own signals of the host molecules but not by the guest redox conversion. This made it possible to decrease the working potential and avoid interference of other species present in biological fluids, e.g., phenylalanine, uric acid and glucose. Simple design and one-step protocol of the sensor assembling are other advantages of the approach proposed. Targeted design of macrocyclic host molecules offers a promising way to possible efficient recognition of other biomolecules on electrochemical detection principles.

CRediT authorship contribution statement

R.V. Shamagsumova: Investigation, Methodology. **T.N. Kulikova:** Investigation. **A.V. Porfireva:** Investigation. **D.N. Shurpik:** Investigation, Methodology. **I.I. Stoikov:** Methodology, Formal analysis. **A.M. Rogov:** Investigation. **D.I. Stoikov:** . **G.A. Evtugyn:** Writing – original draft, Methodology, Supervision.

Data availability

No data was used for the research described in the article.

Declaration of Competing Interest

The authors declare that they have no known competing financial interests or personal relationships that could have appeared to influence the work reported in this paper.

Acknowledgments

Financial support of Russian Science Foundation (grant No 22-13-00070, https://rscf.ru/en/project/22-13-00070) is gratefully acknowledged.

Appendix A. Supplementary data

Supplementary data to this article can be found online at https://doi.org/10.1016/j.jelechem.2023.117444.

References

[1] T. Ogoshi, S. Kanai, S. Fujinami, T. Yamagishi, Y. Nakamoto, para-Bridged symmetrical pillar[5]arenes: their Lewis acid catalyzed synthesis and host-guest property, J. Am. Chem. Soc. 130 (2008) 5022–5023, https://doi.org/10.1021/ja711260m.

[2] T. Ogoshi, T. Yamagishi, Y. Nakamoto, Pillar-shaped macrocyclic hosts pillar[n]arenes: new key players for supramolecular chemistry, Chem. Rev. 116 (2016) 7937–8002, https://doi.org/10.1021/acs.chemrev.5b00765.

[3] T. Ogoshi, T. Kakuta, T. Yamagishi, Applications of pillar[n]arene-based supramolecular assemblies, Angew. Chem. Int. Ed. 58 (2019) 2197–2206, https://doi.org/10.1002/anie.201805884.

[4] Y. Fang, Y. Deng, W. Dehaen, Tailoring pillararene-based receptors for specific metal ion binding: from recognition to supramolecular assembly, Coord. Chem. Rev. 415 (2020) 213313.

[5] Y. Wang, G. Ping, C. Li, Efficient complexation between pillar[5]arenes and neutral guests: from host-guest chemistry to functional materials, Chem. Commun. 52 (2016) 9858–9872, https://doi.org/10.1039/C6CC03999E.

[6] K. Han, Y. Zhang, J. Li, Y. Yu, X. Jia, C. Li, Binding mechanisms and driving forces for the selective complexation between pillar[5]arenes and neutral nitrogen heterocyclic compounds, Eur. J. Org. Chem. 11 (2013) 2057–2060, https://doi.org/10.1002/ejoc.201201647.

[7] S. Ohtani, K. Kato, S. Fa, T. Ogoshi, Host-guest chemistry based on solid-state pillar[n]arenes, Coord. Chem. Rev. 462 (2022) 214503, https://doi.org/10.1016/j.ccr.2022.214503.

[8] P.J. Cragg, Pillar[n]arenes at the chemistry-biology interface, Isr. J. Chem. 58 (2018) 1194–1208, https://doi.org/10.1002/ijch.201800013.

[9] W. Xia, X.-Y. Hu, Y. Chen, C. Lin, L. Wang, A novel redox-responsive pillar[6]arene-based inclusion complex with a ferrocenium guest, Chem. Commun. 49 (2013) 5085–5087, https://doi.org/10.1039/C3CC41903G.

[10] H. Luo, L.-X. Chen, Q.-M. Ge, M. Liu, Z. Tao, Y.-H. Zhou, H. Cong, Applications of macrocyclic compounds for electrochemical sensors to improve selectivity and sensitivity, J. Incl. Phenom. Macrocycl. Chem. 95 (2019) 171–198, https://doi.org/10.1007/s10847-019-00934-6.

[11] S. Cao, L. Zhou, C. Liu, H. Zhang, Y. Zhao, Y. Zhao, Pillararene-based self-assemblies for electrochemical biosensors, Biosens. Bioelectron. 181 (2021) 113164, https://doi.org/10.1016/j.bios.2021.113164.

[12] Y. Acikbas, M. Aksoy, M. Aksoy, D. Karaagac, E. Bastug, A.N. Kursunlu, M. Erdogan, R. Capan, M. Ozmen, M. Ersoz, Recent progress in pillar[n]arene-based thin films on chemical sensor applications, J. Incl. Phenom. Macrocycl. Chem. 100 (2021) 39–54, https://doi.org/10.1007/s10847-021-01059-5.

[13] M. Cheng, W. Gong, M. Lu, J. Ma, Z. Lu, H. Li, Engineering and application of pillar[6]arene functionalized chiral surface in selective adsorption of R adrenaline, Chin. J. Chem. 40 (2022) 925–930, https://doi.org/10.1002/cjoc.20 21 00 714.

[14] H. Zhang, K.-T. Huang, L. Ding, J. Yang, Y.-W. Yang, F. Liang, Electrochemical determination of paraquat using a glassy carbon electrode decorated with pillararene-coated nitrogen-doped carbon dots, Chin. Chem. Lett. 33 (2022) 1537–1540, https://doi.org/10.1016/j.cclet.2021.09.002.

[15] X. Ran, Q. Qu, X. Qian, W. Xie, S. Li, L. Li, L. Yang, Water-soluble pillar[6]arene functionalized nitrogen-doped carbon quantum dots with excellent supramolecular recognition capability and superior electrochemical sensing performance towards TNT, Sens. Actuators B 257 (2018) 362–371, https://doi.org/10.1016/j.snb.2017.10.185.

[16] G. Zhao, X. Zhou, X. Ran, X. Tan, T. Li, M. Cao, L. Yang, G. Du, Layer-by-layer assembly of anionic-/cationic-pillar[5]arenes multilayer films as chiral interface for electrochemical recognition of tryptophan isomers, Electrochemim. Acta 277 (2018) 1–8, https://doi.org/10.1016/j.electacta.2018.04.196.

[17] I. Pisagatti, D. Crisafulli, A. Pappalardo, G.T. Sfrazzetto, A. Notti, F. Nastasi, M.F. Parisi, N. Micali, G. Gattuso, V. Villari, Photoinduced electron transfer in host-guest interactions of a viologen derivative with a didansyl-pillar[5]arene, Mater. Today Chem. 24 (2022) 100841, https://doi.org/10.1016/j.mtchem.2022.100841.

[18] J. Wang, L. Zhou, J. Bei, Q. Zhao, X. Li, J. He, Y. Cai, T. Chen, Y. Du, Y. Yao, An enhanced photo-electrochemical sensor constructed from pillar[5]arene functionalized Au NPs for ultrasensitive detection of caffeic acid, Talanta 243 (2022) 123322, https://doi.org/10.1016/j.talanta.2022.123322.

[19] X. Tan, T. Mu, S. Wang, J. Li, J. Huang, H. Huang, Y. Pua, G. Zhao, Simultaneous determination of acetaminophen and dopamine based on a water-soluble pillar[6]arene and ultrafine Pd nanoparticle modified covalent organic framework nanocomposite, Analyst 146 (2021) 262–269, https://doi.org/10.1039/d0an01717e.

[20] T.-B. Wei, J.-F. Chen, B. Xi, H. Cheng, B.-B. Li, Y.-M. Han, H. Zhang, Q.L. Yao, A novel functionalized pillar[5]arene-based selective amino acid sensor for L-tryptophan, Org. Chem. Front. 4 (2017) 210–213, https://doi.org/10.1039/c6qo00569a.

[21] Y.-M. Zhang, Q.-Y. Yang, X.-Q. Ma, H.-Q. Dong, Y.-F. Zhang, W.-L. Guan, H. Yao, T.-B. Wei, Q. Lin, N-(2-aminoethyl)-2-(hexylthio) acetamide-functionalized pillar[5]arene for the selective detection of l-trp through guest-adaptive multisupramolecular interactions, J. Phys. Chem. A 124 (2020) 9811–9817, https://doi.org/10.1021/acs.jpca.0c08367.

[22] R. Zhang, Y. Ren, Q. Zhang, W. Huang, H. Bai, X. Zeng, Water-soluble pillar[5]arene-modified graphdiyne functional material and its application towards ultrasensitive and robust electrochemical methylamphetamine determination, New J. Chem. 46 (2022) 20909–20917, https://doi.org/10.1039/D2NJ03668A.

[23] H. Zhao, W. Xie, R.-L. Zhang, X.-D. Wang, H.-F. Liu, J. Li, T. Sha, X.-S. Guo, J. Li, Q.-M. Sun, Y.-P. Zhang, C.-P. Li, Electrochemical sensor for human norovirus based on covalent organic framework/pillararene heterosupramolecular nanocomposites, Talanta 237 (2022) 122896, https://doi.org/10.1016/j.talanta.2021.122896.

[24] F. Guo, P. Xiao, B. Yan, M. Hahn, Y. Kong, W. Zhang, Y. Piao, G. Diao, One-pot synthesis of hydrazide-pillar[5]arene functionalized reduced graphene oxide for supercapacitor electrode, Chem. Eng. J. 391 (2020) 123511, https://doi.org/10.1016/j.cej.2019.123511.

[25] F. Guo, J. Guo, Z. Zheng, T. Xia, A.N. Chishti, L. Lin, W. Zhang, G. Diao, Polymerization of pyrrole induced by pillar[5]arene functionalized graphene for supercapacitor electrode, Chinese Chem. Lett. 33 (2022) 4846–4849, https://doi.org/10.1016/j.cclet.2022.01.088.

[26] W. Zhang, J. Yang, X. Li, T. Chen, S. Park, M. Bae, D. Jung, L. Lin, S.H. Paek, Y. Piao, Anticancer pH-responsive supramolecular vesicles fabricated using water-soluble pillar[5]arene and curcumin derivative, Mater. Design. 222 (2022) 111084, https://doi.org/10.1016/j.matdes.2022.111084.
[27] D.N. Shurpik, A.A. Akhmedov, P.J. Cragg, V.V. Plemenkov, I.I. Stoikov, Progress in the chemistry of macrocyclic meroterpenoids, Plants 9 (2020) 1582, https://doi.org/10.3390/plants9111582.
[28] G.A. Evtyugin, D.N. Shurpik, I.I. Stoikov, Electrochemical sensors and biosensors on the pillar[5]arene platform, Russ. Chem. Bull. 69 (2020) 859–874, https://doi.org/10.1007/s11172-020-2843-2.
[29] I.I. Stoikov, P.L. Padnya, O.A. Mostovaya, A.A. Vavilova, V.V. Gorbachuk, D.N. Shurpik, G.A. Evtugin, Macrocycle-based oligo- and polylactides: synthesis and prospects of application, Russ. Chemi. Bull. 68 (2019) 1962–1982, https://doi.org/10.1007/s11172-019-2655-4.
[30] S. Yang, L. Liu, M. You, F. Zhang, X. Liao, P. He, The novel pillar[5]arene derivative for recyclable electrochemical sensing platform of homogeneous DNA hybridization, Sens. Actuators B 227 (2016) 497–503, https://doi.org/10.1016/j.snb.2015.12.090.
[31] X. Qian, H. Yang, S. Liu, L. Yang, J. Li, W. Gao, G. Du, Q. Qu, X. Ran, Supramolecular DNA sensor based on the integration of host-guest immobilization strategy and WP5-Ag/PEHA supramolecular aggregates, Anal. Chim. Acta 1220 (2022) 340077, https://doi.org/10.1016/j.aca.2022.340077.
[32] X. Zhou, L. Yang, X. Tan, G. Zhao, X. Xie, G. Du, A robust electrochemical immunosensor based on hydroxyl pillar[5]arene@AuNPs@g-C_3N_4 hybrid nanomaterial for ultrasensitive detection of prostate specific antigen, Biosens. Bioelectron. 112 (2018) 31–39, https://doi.org/10.1016/j.bios.2018.04.036.
[33] X. Qian, X. Zhou, Q. Qu, L. Li, L. Yang, Ultrasensitive and robust electrochemical sensing platform for the detection of squamous cell carcinoma antigen using water-soluble pillar[5]arene-Pd/MoS_2 nanocomposites, Electrochim. Acta 313 (2019) 235–244, https://doi.org/10.1016/j.electacta.2019.05.032.
[34] J. Wang, J. Bei, X. Guo, Y. Ding, T. Chen, B. Lu, Y. Wang, Y. Du, Y. Yao, Ultrasensitive photoelectrochemical immunosensor for carcinoembryonic antigen detection based on pillar[5]arene-functionalized Au nanoparticles and hollow PANI hybrid BiOBr heterojunction, Biosens. Bioelectron. 208 (2022) 114220, https://doi.org/10.1016/j.bios.2022.114220.
[35] V.A. Smolko, D.N. Shurpik, R.V. Shamagsumova, A.V. Porfireva, V.G. Evtugyn, L.S. Yakimova, I.I. Stoikov, G.A. Evtugyn, Electrochemical behavior of pillar[5]arene on glassy carbon electrode and its interaction with Cu^{2+} and Ag^{+} ions, Electrochim. Acta 147 (2014) 726–734, https://doi.org/10.1016/j.electacta.2014.10.007.
[36] R.V. Shamagsumova, D.N. Shurpik, Y.I. Kuzin, I.I. Stoikov, A.M. Rogov, G.A. Evtugyn, Pillar[6]arene: electrochemistry and application in electrochemical (bio) sensors, J. Electroanal. Chem. 913 (2022) 116281, https://doi.org/10.1016/j.jelechem.2022.116281.
[37] V. Smolko, D. Shurpik, V. Evtugyn, I. Stoikov, G. Evtugyn, Organic acid and DNA sensing with electrochemical sensor based on carbon black and pillar[5]arene, Electroanalysis 28 (2016) 1391–1400, https://doi.org/10.1002/elan.201501080.
[38] T. Ogoshi, Y. Hasegawa, T. Aoki, Y. Ishimori, S. Inagi, T. Yamagishi, Reduction of emeraldine base form of polyaniline by pillar[5]arene based on formation of poly (pseudorotaxane) structure, Macromolecules 44 (2011) 7639–7644, https://doi.org/10.1021/ma2016979.
[39] H. Saba, J. An, Y. Yang, M. Xue, Y. Liu, Voltammetric behavior of 1,4-dimethoxypillar[m]arene[n]quinones, Chin. J. Chem. 34 (2016) 861–865, https://doi.org/10.1002/cjoc.201600282.
[40] M.R. Avei, S. Etezadi, B. Captain, A.E. Kaifer, Visualization and quantitation of electronic communication pathways in a series of redox active pillar[6]arene-based macrocycles, Commun. Chem. 3 (2020) 117, https://doi.org/10.1038/s42004-020-00363-4.
[41] T. Hirohata, S. Tomoki, U. Naoki, Y. Hidehiro, N. Nobuhiro, H. Nishihara, T. Ogoshi, I. Tomita, S. Inagi, Pillar[6]quinone: facile synthesis, crystal structures and electrochemical properties, Chem. Commun. 57 (2021) 6360–6363, https://doi.org/10.1039/D1CC02413B.
[42] J. Wang, M. Cen, J. Wang, D. Wang, Y. Ding, G. Zhu, B. Lu, X. Yuan, Y. Wang, Y. Yao, Water-soluble pillar[4]arene[1]quinone: synthesis, host-guest property and application in the fluorescence turn-on sensing of ethylenediamine in aqueous solution, organic solvent and air, Chinese Chem. Lett. 33 (2022) 1475–1478, https://doi.org/10.1016/j.cclet.2021.08.044.
[43] M. Dehabadi, E. Yemisci, A.N. Kursunlu, D. Kirsanov, Novel pillar[5]arenes show high cross-sensitivity in PVC-plasticized membrane potentiometric sensors, Chemosensors 10 (2022) 420, https://doi.org/10.3390/chemosensors10100420.
[44] E. Li, K. Jie, Y. Zhou, R. Zhao, B. Zhang, Q. Wang, J. Liu, F. Huang, Aliphatic aldehyde detection and adsorption by nonporous adaptive pillar[4]arene[1]quinone crystals with vapochromic behavior, ACS Appl. Mater. Interfaces 10 (2018) 23147–23153, https://doi.org/10.1021/acsami.8b06396.
[45] D.N. Shurpik, P.L. Padnya, L.I. Makhmutova, L.S. Yakimova, I.I. Stoikov, Selective stepwise oxidation of 1,4-decamethoxypillar[5]arene, New J. Chem. 39 (2015) 9215–9220, https://doi.org/10.1039/C5NJ01951F.
[46] Y. Yao, M. Xue, X. Chi, Y. Ma, J. He, Z. Abliz, F. Huang, A new water-soluble pillar[5]arene: synthesis and application in the preparation of gold nanoparticles, Chem. Commun. 48 (2012) 6505–6507, https://doi.org/10.1039/C2CC31962D.
[47] E. Laviron, General expression of the linear potential sweep voltammogram in the case of diffusionless electrochemical systems, J. Electroanal. Chem. Inter. Electrochem. 101 (1979) 19–28, https://doi.org/10.1016/S0022-0728(79)80075-3.
[48] P.S. Guin, S. Das, P.C. Mandal, Electrochemical reduction of quinones in different media: a review. Int. J. Electrochem. (2011) 816202. doi: 10.4061/2011/816202.
[49] M. Quan, D. Sanchez, M.F. Wasylkiw, D.K. Smith, Voltammetry of quinones in unbuffered aqueous solution: reassessing the roles of proton transfer and hydrogen bonding in the aqueous electrochemistry of quinones, J. Am. Chem. Soc. 129 (2007) 12847–12856, https://doi.org/10.1021/ja0743083.
[50] X. Ji, C.E. Banks, D.S. Silvester, A.J. Wain, R.G. Compton, Electrode kinetic studies of the hydroquinone - benzoquinone system and the reaction between hydroquinone and ammonia in propylene carbonate: Application to the indirect electroanalytical sensing of ammonia. J. Phys. Chem. C 111 (2007) 1496-1504. doi: 0.1021/jp066704y.
[51] F. Arduini, S. Cinti, V. Mazzaracchio, V. Scognamiglio, A. Amine, D. Moscone, Carbon black as an outstanding and affordable nanomaterial for electrochemical (bio)sensor design, Biosens. Bioelectron. 156 (2020) 112033, https://doi.org/10.1016/j.bios.2020.112033.
[52] A.J. Bard, L.R. Faulkner, Electrochemical Methods. Fundamentals and Applications, J. Willey & Sons, New York, 1980.
[53] A.J. Gelenberg, C.J. Gibson, J.D. Wojcik, Neurotransmitter precursors for the treatment of depression, Psychopharmacol. Bull. 18 (1982) 7–18. PMID: 10696120.
[54] C. Deng, Y. Deng, B. Wang, X. Yang, Gas chromatography–mass spectrometry method for determination of phenylalanine and tyrosine in neonatal blood spots, J. Chromatogr. B 780 (2002) 407–413, https://doi.org/10.1016/S1570-0232(02)00632-3.
[55] R. Kand'ár, P. Žáková, Determination of phenylalanine and tyrosine in plasma and dried blood samples using HPLC with fluorescence detection, J. Chromatogr. B 877 (30) (2009) 3926–3929.
[56] Y. Huang, X. Jiang, W. Wang, J. Duan, G. Chen, Separation and determination of l-tyrosine and its metabolites by capillary zone electrophoresis with a wall-jet amperometric detection, Talanta 70 (2006) 1157–1163, https://doi.org/10.1016/j.talanta.2006.03.009.
[57] F. Wibrand, A microplate-based enzymatic assay for the simultaneous determination of phenylalanine and tyrosine in serum, Clin. Chim. Acta 347 (2004) 89–96, https://doi.org/10.1016/j.cccn.2004.04.012.
[58] K. Moulaee, G. Neri, Electrochemical amino acid sensing: a review on challenges and achievements, Biosensors 11 (2021) 502, https://doi.org/10.3390/bios11120502.
[59] A. Dinu, C. Apetrei, A review of sensors and biosensors modified with conducting polymers and molecularly imprinted polymers used in electrochemical detection of amino acids: phenylalanine, tyrosine, and tryptophan, Int. J. Mol. Sci. 23 (2022) 1218, https://doi.org/10.3390/ijms23031218.
[60] J. Hongpaisan, G.M. Roomans, Retaining ionic concentrations during in vitro storage of tissue for microanalytical studies, J. Microscopy 193 (1999) 257–267, https://doi.org/10.1046/j.1365-2818.1999.00461.x.